# EVALUATION OF THE OMI AEROSOL INDEX USING COINCIDENT LIDAR OBSERVATIONS

**Vassilis Amiridis, Elina Giannakaki, Mariliza Koukouli, Stylianos Kazadzis, Dimitris Balis and Alkis Bais**

*Laboratory of Atmospheric Physics, Aristotle University of Thessaloniki, Thessaloniki 54124, Greece,*
*e-mail: vamoir@auth.gr*

## ABSTRACT

A three-month observational campaign, combining OMI/Aura overpasses with coordinated synchronous detailed sunphotometer, cloud cover and lidar measurements took place in summer 2005 at Thessaloniki Greece (40.5$^o$N, 22.9$^o$E) in order to evaluate the UV and aerosol products of OMI. Here we present comparisons of the aerosol index with lidar measurements, giving emphasis to the free tropospheric aerosol load and the lidar ratio. There are indications for a positive correlation between lidar ratio and aerosol index, while the highest aerosol index and aerosol optical depth values were found for air masses originating from the Sahara desert.

## 1. INTRODUCTION

Aerosols over the Mediterranean basin result from the superimposition of a marine component, a mineral dust component and an anthropogenic component [1, 2, 3, 4, 5]. The atmosphere above Thessaloniki, located in the northern Aegean Sea region, is hence affected by aerosols originating both from local and regional pollution sources, Saharan dust outbusts, long-range transport of biomass burning particles and maritime particles [6, 7, 8, 9]. Among these particles, sea-spray and sulphate aerosols are the most common non-absorbing aerosols [10], whereas carbonaceous (smoke) particles can have both absorbing and non-absorbing characteristics [10] and mineral or dust aerosols, transported from nearby dry regions, represent the clearest main absorbing signature [11].
The Absorbing Aerosol Index [AI] [10] is a measure of the reduction of the Rayleigh scattered radiance by aerosol absorption relative to a pure Rayleigh scattered radiance, studied via its wavelength dependence. As expected, different types of aerosols leave a distinct signature in the observed spectrum. When UV absorbing aerosols are present in the atmosphere aerosol index is positive while non-absorbing aerosols produce a negative aerosol index.

## 2. INSTRUMENTATION AND METHODS

A 355 nm Raman lidar is used to perform continuous measurements of suspended aerosol particles in the planetary boundary layer (PBL) and the lower free troposphere (FT), is located at the Laboratory of Atmospheric Physics (LAP). It is based on the second and third harmonic frequency of a compact, pulsed Nd:YAG laser, which emits pulses of 300 and 120 mJ at 532 nm and 355 nm, respectively, with a 10Hz repetition rate [12]. The optical receiver is a 500 nm diameter telescope. In this study we use daytime backscatter measurements combined with aerosol optical depth measurements performed using a UV spectrophotometer, in order to estimate with the lidar the profile of the extinction coefficient and a constant with height estimate of the lidar ratio. The lidar ratio estimates have been successfully evaluated with corresponding night time measurements of LR of the same day, when available.

Analytical backward trajectories provide information about the origin of the observed aerosols and about the synoptic patterns corresponding to the measurements. For the purpose of this work, four-day back trajectories were computed for the days of interest, using Hybrid Single-Particle Lagragian Integrated Trajectory (HYSPLIT) model [13]. We used HYSPLIT to generate 4-day back trajectories for air-parcels arriving over Thessaloniki site at altitudes from 500m to 6000m. The analytical back-trajectories were calculated for an arrival time of 12:00 UTC.

## 3. RESULTS AND DISCUSSION

From the three months campaign (1 July – 30 September 2005) we selected 22 coincident OMI overpass data and lidar measurements, within 1 hour using only data with low reflectivity (<20%), in order to avoid the effect of cloud cover in the comparisons. In addition, the probed air-masses have been characterized according to their origin, using the 4-day back-trajectories described in the previous paragraph. From this analysis we identified four clusters in our data, namely the NNE sector which corresponds to air masses originating from Eastern Europe, SW, which corresponds to air masses mostly originating from Sahara desert, NNW, which correspond to air masses mostly advected from central Europe and finally WNW which corresponds to air masses originating from Italy, Spain and possibly the Atlantic Ocean. Fig. 1 shows a scatter plot between the optical depths estimated with the lidar, as an integral of the aerosol extinction profiles, versus the aerosol index from OMI. Different symbols

indicate different origin of the air masses. As it is indicated in Fig.1 for the NNE originating aerosols the aerosol index is close to zero (showing also negative values), while there is a large variability of the optical depth. This fact provides an indication that these aerosols are less absorbing or even non-absorbing. For the WNW and NNW clusters it seems that there is a correlation between the optical depth and the aerosol index, indicating absorbing aerosol layers at a height detectable from OMI. Concerning the Sahara dust cases it is interesting to note that the lidar estimates of the aerosol optical depth at 355nm are almost constant around 0.6, while the aerosol index shows variable positive large values between 1 and 3.

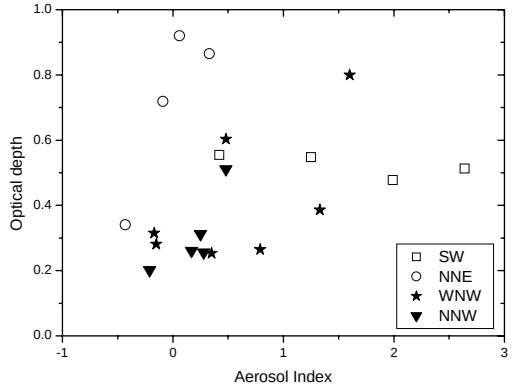


**Fig.1.** Aerosol optical depth at 355nm versus the OMI aerosol index for Thessaloniki. Different symbols indicate different origin of the air masses

It is well established in the literature that the aerosol index depends much on the height of the aerosol layer in addition to the optical depth and aerosol type [14]. In order to explain the aerosol behaviour for the Sahara dust cases, we examined separately the dependence of the aerosol index on the free tropospheric fraction of the aerosol optical depth at 355nm (here defined as the integral above 2km). The corresponding scatter plot is presented in Fig. 2. In general it is evident from this figure that there is a positive correlation between the free tropospheric aerosol loading and the aerosol index. This correlation is more pronounced for the Saharan dust cases, where we also indicate on the plot the height of the desert dust layers. The thickest and highest free tropospheric desert dust layers give the largest aerosol index values. There is only an exception in Fig.2 where the dust case with AI close to 3 is at a rather low altitude. This can be due to the presence of absorbing particles below the desert dust, which are however detectable by OMI.

The lidar ratio provides a measured indication of the type of the aerosols [15]. In addition, Hsu et. al. [14] have shown that the sensitivity of the aerosol index in TOMS data highly depends on the type of the aerosols considered (apart from the height and the aerosol optical depth). Therefore we examined the possible dependence between the aerosol index and the lidar ratio. The results are presented in Fig. 3.

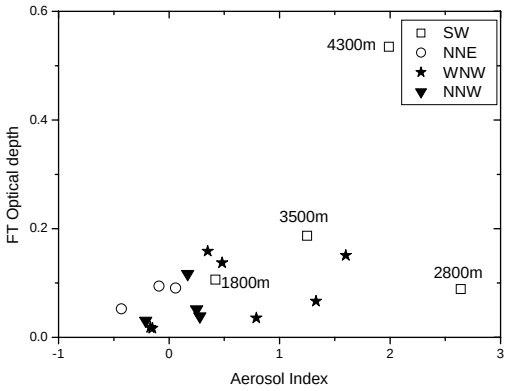


**Fig.2.** Aerosol optical depth of the free troposphere at 355nm versus the OMI aerosol index for Thessaloniki. Different symbols indicate different origin of the air masses

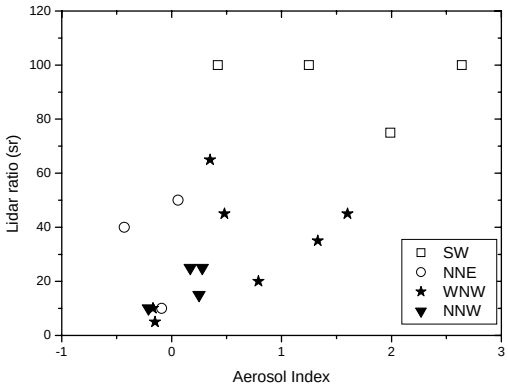


**Fig.3.** Mean lidar ratio at 355nm versus the OMI aerosol index for Thessaloniki. Different symbols indicate different origin of the air masses

Fig. 3 indicates a positive correlation between the lidar ratio and the OMI aerosol index. Small lidar ratios which correspond for Thessaloniki mostly to maritime aerosols [12] show small aerosol index values as a result of less absorbing aerosols. Larger lidar ratio values that correspond mostly to polluted continental aerosols or desert dust correspond to the largest aerosol index values observed. The small variation in the lidar ratio value (of the order of 20sr) for the case of 4300m data point is not an indication of different type of aerosol, especially when the lidar ratios are of the order of ~90sr. Lidar ratio values are not expected to be affected by the possible enhancement of the columnar absorption from the boundary layer aerosols in the cases where the Saharan dust plumes are mainly affecting the scattering

properties. This analysis is of course indicative and it will require more data to be statistically significant.

Fig. 4 presents a classification of aerosol optical properties (namely AI, AOD and LR) in dependence on the large-scale weather regime. The main clusters were determined from a cluster analysis algorithm applied to back-trajectories for the days of our interest.

The lowest mean AOD values (0.257±0.04) correspond to NNW cluster which represents fast transport from the Atlantic Ocean. For this cluster also the AI takes minimum values (0.123±0.22) indicating less absorbing aerosols. For these days, the free tropospheric AOD according to our backscatter lidar measurements contributed approximately 15% to the total AOD.

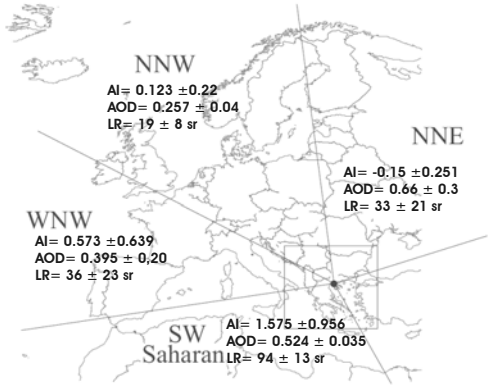


**Fig 4.** Average aerosol properties of the aerosol during summer 2005 over Thessaloniki relative to the origin of the observed air-masses.

Similar studies [15] show that the single scattering albedo for this cluster indicates the presence of more absorbing aerosols. It is believed that the possibly absorbing boundary layer aerosols from local sources (which are dominating the main aerosol load for this cluster) are also affecting the effective ssa. For this cluster, the AI may fail to represent more absorbing characteristics of Thessaloniki's boundary layer aerosol load, since any aerosol below about 1000m is unlikely to be detected [14]. Higher AOD, AI and LR values are associated with the WNW cluster, following the increasing free-tropospheric contribution to the total AOD observed for these days. The correlation between the free tropospheric AOD and the AI (Fig. 2) is better for this cluster, since higher aerosol layers are better detectable by OMI. The lowest AI values are associated with the NNE originating aerosols (showing also negative values), while there is a large variability of the optical depth. NNE flow transports pollution from the Balkans and Eastern Europe and during summer is associated with regions with large emissions from biomass burning episodes. Single scattering albedo values estimated by Balis et. al. [15] for aerosols with the same origin were 0.95±0.3. Free tropospheric contribution was found to be significant for this cluster and the AI measurements are consistent with the ssa estimates, indicating less absorbing aerosols for this cluster. Finally, the SW cluster which is mostly associated with Saharan dust transport is related with higher free tropospheric contribution to the total AOD and the absorbing features of dust are better represented by the AI.

## 4. SUMMARY AND CONCLUSIONS

In this paper we presented comparisons of the OMI aerosol index with lidar measurements, giving emphasis to the free tropospheric aerosol load and the lidar ratio. Measurements performed during a three-month observational campaign were analyzed, in order to investigate the potential of the AI to characterize absorption aerosol features in the case of Thessaloniki, which its atmosphere hosting a mixture of different types of aerosol particles. It was found that the sensitivity of the aerosol index to aerosols increases about proportionally with aerosol layer height. The highest aerosol index and aerosol optical depth values were found for air masses originating from the Sahara desert. The thickest and highest desert dust layers give larger aerosol index values. A classification of optical aerosol properties in dependence on the large-scale weather regime showed that for the case of NNE flows where free tropospheric contribution is significant, the AI indicates less absorbing aerosols. For cluster associated with Westerly flows the AI is well correlated with the AOD showing however possibly underestimated absorption features according to relative studies. Finally, there are indications for a positive correlation between lidar ratio and aerosol index.

## ACKNOWLEDGMENTS

OMI aerosol index data have been extracted from http://toms.gsfc.nasa.gov. Air mass back trajectories were calculated with the Hybrid Single-Particle Lagrangian Integrated Trajectory model (NOAA). VA acknowledges the support of the Greek Ministry of Education (Pythagoras EPEAEK-2 project). EG acknowledges the support of the GSRT-PENED project. SK acknowledges the support of IKY Foundation.

## REFERENCES

1. Moulin C., et al., Control of atmospheric export of dust from North Africa by the North Atlantic oscillation, *Nature*, Vol. 387, 691-694, 1997.

2. Zerefos C., et. al., On the origin of $SO_2$ above Northern Greece, *Geophys. Res. Lett.*, Vol. 27, 365-368, 2000.

3. Lelieveld J., et al., Global air pollution crossroads over the Mediterranean, *Science*, Vol. 298, 794-799, 2002.

4. di Sarra A., et al. Desert aerosol in the Mediterranean, in: Mediterranean Climate: Variability and Trends, edited by: *Bolle, H-J*, Spinger-Verlag, 309-315, 2003
5. Barnaba F. and Gobbi G.P., Aerosol seasonal variability over the Mediterranean region and relative impact of maritime, continental and Saharan dust particles over the basin from MODIS data in the year 2001, *Atm Chem Phys*, Vol. 4, 2367-2391, 2004.
6. Gerasopoulos E., et. al., Climatological aspects of aerosol optical properties in Nothern Greece, *Atmos Chem Phys*, Vol. 3, 2025-2041, 2003.
7. Balis D. S., et. al., Raman lidar and sunphotometric measurements of aerosol optical properties over Thessaloniki, Greece during a biomass burning episode, *Atm. Env.*, Vol. 37, 4529-4538, 2003.
8. Balis D. S., et. al., Study of the effect of different type of aerosols on UV-B radiation from measurements during EARLINET, *Atmos.Chem.Phys.*, Vol. 4, 1-15, 2004.
9. Papayannis A., et. al., Measurements of Saharan dust aerosols over the Eastern Mediterranean using elastic backscatter-Raman lidar, spectrophotometric and satellite observations in the frame of the EARLINET project, *ACPD*, Vol. 5, 2075-2110, 2005.
10. Torres O., et. al., Derivation of aerosol properties from satellite measurements of backscatter ultraviolet radiation: Theoretical basis, *J. Geophys. Res.*, Vol. 103, 17,099-17,110, 1998.
11. Israelevich PL., et. al., Desert aerosol transport in the Mediterranean region as inferred from the TOMS aerosol index", *J. Geophys. Res.*,107**,** 4572, 2002.
12. Amiridis V., et. al., Four-year aerosol observations with a Raman lidar at Thessaloniki, Greece, in the framework of EARLINET, *J. Geophys. Res.,* vol. 110, d21203, doi: 10.1029/2005JD006190, 2005.
13. Draxler, R.R. and G.D. Hess, Description of the HYSPLIT_4 modeling system, NOAA Tech. Memo. ERL ARL-224,24, 1997.
14. Hsu NC., et. al., Comparisons of the TOMS aerosol index with Sun-photometer aerosol optical thickness: Results and applications, *J. Geophys. Res.*, 104, 6269-6279, 1999.
15. Balis et. al., Characterization of the aerosol type using simultaneous measurements of the lidar ratio and the single scattering albedo during EARLINET (2001-2004), in Geophysical Research Abstracts Vol. 7, European Geosciences Union, General Assembly, April 24-29, Vienna, Austria, EGU05-A-03039, 2005.